Journal of the Korean Magnetic Resonance Society **2020**, *24*, 70-76
DOI 10.6564/JKMRS.2020.24.3.070

Backbone NMR assignments of the anti-CRISPR AcrIIA5 from phages infecting *Streptococcus thermophilus*

So Young An[1], Eun-Hee Kim[2], Euiyoung Bae[1], and Jeong-Yong Suh[1,*]

[1]Department of Agricultural Biotechnology and Research Institute of Agriculture and Life Sciences, Seoul National University, Seoul 08826, Republic of Korea,
[2]Center for Research Equipment, Korea Basic Science Institute, Ochang 28119, Republic of Korea

Received Sep 10, 2020; Revised Sep 17, 2020; Accepted Sep 17, 2020

Abstract The CRISPR-Cas system provides an adaptive immunity for bacteria and archaea against invading phages or foreign plasmids. In the type II CRISPR-Cas system, a single effector protein Cas9 and a guide RNA form an RNA-guided endonuclease complex that can degrade DNA targets of foreign origin. To avoid the Cas9-mediated destruction, phages evolved anti-CRISPR (Acr) proteins that neutralize the host bacterial immunity by inactivating the CRISPR-Cas system. Here we report the backbone ^{1}H, ^{15}N, and ^{13}C resonance assignments of AcrIIA5 that inhibits the endonuclease activity of type II-A *Streptococcus thermophilus* Cas9 and also *Streptococcus pyogenesis* Cas9 using triple resonance nuclear magnetic resonance spectroscopy. The backbone chemical shifts of AcrIIA5 predict a disordered region at the N-terminus, followed by an αββββαβββ fold.

Keywords AcrIIA5, anti-CRISPR, Cas9, NMR spectroscopy

Introduction

The clustered regularly interspaced short palindromic repeats (CRISPR) and CRISPR-associated (Cas) proteins constitute an adaptive immunity of bacteria and archaea against bacteriophages and foreign plasmids [1, 2]. Upon infection, bacteria activates the CRISPR-Cas system to integrate short segments (spacers) of invading nucleic acids into the CRISPR loci of the host genome. Upon subsequent invasion, CRISPR RNA (crRNA) and sometimes trans-activating CRISPR RNA (tracrRNA) as well are transcribed and processed to associate with Cas proteins, and the RNA-guided endonuclease complex recognizes and destroys nucleic acids that are complementary to the guide sequence of crRNA. The CRISPR-Cas systems are divided into two classes based on the nature of the interference complex (multiple subunits or a single effector), and further into various types and subtypes according to the phylogenic and genetic signature[3]. *Streptococcus pyogenes* Cas9 (SpyCas9) belongs to the subtype II-A of the Class2 CRISPR-Cas system. SpyCas9 has been extensively investigated and applied to genome editing due to its simplicity in targeting double-strand DNA at desired sites guided by single-guide RNA (sgRNA)[4-6].

Arms-race between bacteria and phages have long been evolved, developing a variety of arsenal to compete for invasion and defense[7]. Recently AcrIIA5 encoded by virulent phages infecting *Streptococcus*

* Address correspondence to: **Jeong-Yong Suh,** Department of Agricultural Biotechnology and Research Institute of Agriculture and Life Sciences, Seoul National University, Seoul 08826, Republic of Korea, Tel: 82-2-880-4879; E-mail: jysuh@snu.ac.kr

thermophilus prophages have shown a wide inhibitory activity against different Cas9 proteins including SpyCas9, highlighting their potential as an off-switch for Cas9 to control gene editing[8]. Biochemical and cell-based assays have been employed to reveal that AcrIIA5 inhibits a broad range of Cas9 orthologs, preventing the cleavage of target DNA[9,10]. Here we report the backbone chemical shifts and secondary structures of AcrIIA5 using triple-resonance NMR spectroscopy.

Experimental Methods

Sample preparation- The synthetic AcrIIA5 (a.a. 1–140) gene was cloned into a pET28 vector with an N-terminal His_6-tag and a maltose binding protein (MBP) tag, and verified by DNA sequencing. The plasmid was introduced into *Escherichia coli* strain BL21star(DE3) cells (Invitrogen), and grown minimal media with $^{15}NH_4Cl$ and/or $^{13}C_6$-glucose as sole nitrogen or carbon sources, respectively. Cells were grown at 37°C to OD_{600} 0.6~0.8, induced with 1 mM isopropyl-β-D-thiogalactopyranoside (IPTG) at 18°C, and harvested by centrifugation after 20 hours of induction. Cell pellets were resuspended in 20 mM Tris-HCl, pH 7.4, 500 mM NaCl, 5% glycerol, 5 mM β-mercaptoethanol (buffer A) with 1 mM phenylmethylsulfonyl-fluoride(PMSF), lysed using Emulsiflex C3 (AVESTIN) and centrifuged at 40,000 g for 30 min. The clear supernatant was loaded onto a HisTrap column (GE Healthcare) equilibrated with buffer A and eluted with 500 mM imidazole. The His_6-tag and maltose binding protein (MBP) was removed using TEV protease in buffer A with 0.5 mM EDTA, and the digestion reaction was loaded onto the SP column(GE Healthcare) and eluted with a 0−1 M NaCl gradient. The flow-through was collected and loaded onto a Superdex 75 column (GE Healthcare) equilibrated with buffer A.

NMR experiments - The NMR sample contained 0.6 mM ^{13}C,^{15}N-AcrIIA5 in with 10 mM sodium phosphate, pH 7.0, 500 mM NaCl, 5 mM β-mercaptoethanol and 10% D_2O. NMR spectra were recorded at 25°C on 900 MHz spectrometers equipped with a z-shielded gradient triple resonance probe. Sequential backbone assignments of ^1H, ^{15}N and ^{13}C resonances were achieved by three-dimensional triple resonance through-bond scalar correlation experiments CBCA(CO)NH, HNCACB, HNCO, HN(CA)CO, NMR spectra were processed using the NMRPipe[11], and analyzed using PIPP[12], and NMRView[13] programs. Overall secondary structure and the backbone dihedral torsion angles were predicted from TALOS+ based on combined H_N, ^{15}N, Cα, Cβ and C' backbone chemical shifts[14].

Results and Discussion

Backbone assignment of AcrIIA5- AcrIIA5 has 140 amino acids and exhibited a well dispersed 2D ^1H–^{15}N HSQC NMR spectrum (Figure 1A). We noticed that the HSQC spectra of ^{15}N-labeled AcrIIA5 in 20 mM Tris, pH 7.4, showed fewer backbone amide resonances than expected. When we changed the buffer to 10 mM sodium phosphate, pH 7.0, a dozen of new resonances appeared (Figure 1A). Thus, we used pH 7.0 for the sequential backbone assignment of AcrIIA5, and obtained a suite of three-dimensional heteronuclear correlation NMR spectroscopy, such as HNCO, HN(CA)CO, CBCA(CO)NH, and HNCACB, using a standard protocol[15,16]. The backbone chemical shifts for 118 out of 140 residues were assigned, and the residues without assignments did not appear in the 2D ^1H-^{15}N HSQC spectra, suggesting a line broadening by conformational exchanges.

Amino-acid selective isotope labeling is often useful to resolve ambiguous assignments. It has also been reported that reverse isotope labeling can help assignments by selectively filtering out resonances of particular amino acids. We tried the reverse isotope labeling of Leu to help the assignment of AcrIIA5. Briefly, $^{15}NH_4Cl$ was used in the same manner as the uniform 15N-labeling protocol, and in addition, 50 mg of unlabeled leucine was introduced before induction to dilute the isotope-labeling of leucine positions.[17] The reverse labeling of Leu indeed suppressed the peak intensity of Leu resonances (Figure 1B).

However, resonances of other aliphatic amino acids also appeared with reduced intensity, possibly from scrambling of biosynthetic pathways. For example, Ile117 and Ala119, among others, exhibited lower intensity compared to those from uniformly ^{15}N-labeled AcrIIA5 (Figure 1B). Nevertheless, clarification of Leu residues with a long spin system facilitated fast and reliable backbone assignment. The ^{1}H, ^{15}N and ^{13}C chemical shifts from the backbone assignment of AcrIIA5 are listed in Table 1, and the annotated HSQC spectrum is shown in Figure 2.

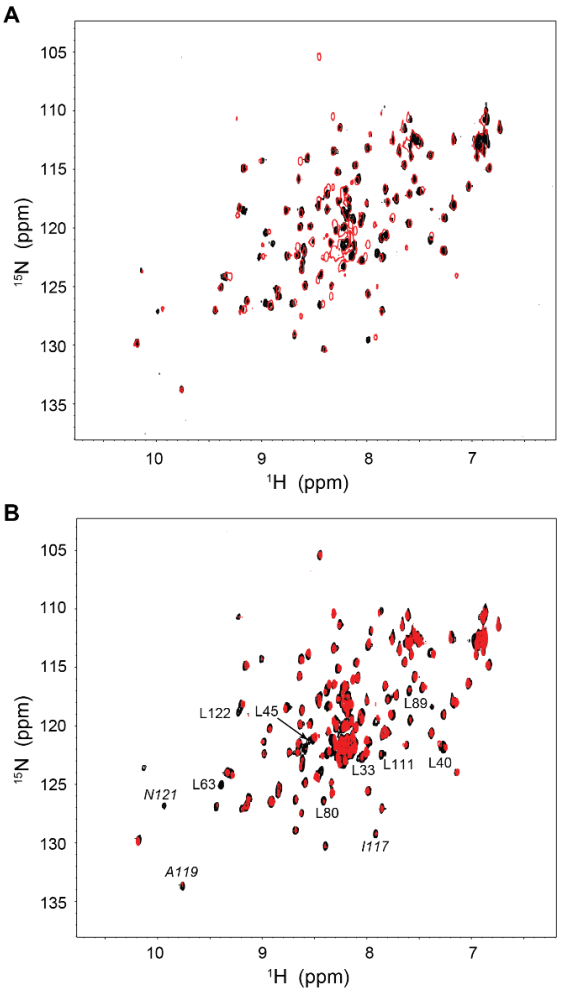

Figure 1. (A) The superimposed ^{1}H–^{15}N HSQC spectra of ^{15}N-AcrIIA5 in pH 7.4 (black) and pH 7.0 (red). (B) The superimposed ^{1}H–^{15}N HSQC spectra of uniformly ^{15}N-labeled AcrIIA5 (black), and Leu-reverse-labeled AcrIIA5 (red).

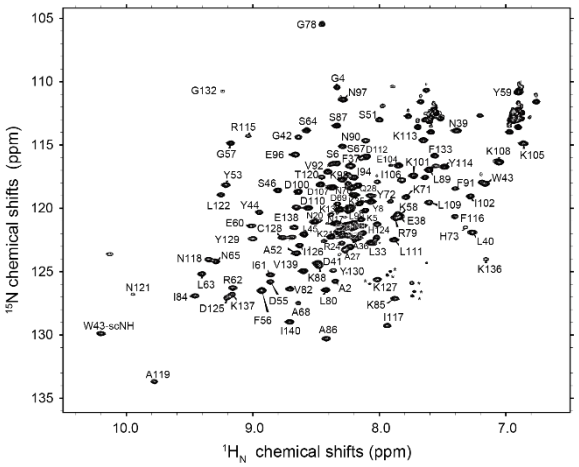

Figure 2. ^{1}H–^{15}N HSQC spectra of ^{15}N-AcrIIA5 with backbone chemical shift assignments obtained by triple-resonance heteronuclear NMR experiments.

Disorder prediction of AcrIIA5- We noticed that the several backbone amide resonances in the HSQC spectrum appeared in the narrow range between 8 ppm and 8.5 ppm of the ^{1}H chemical shifts, which is typical of a disordered region. We examined if the amino acid sequence of AcrIIA5 would have the characteristic of intrinsically disordered region. We employed two prediction programs, PONDR and IUPred2, to assess the disorder score of AcrIIA5 (Figure 3)[18,19]. Interestingly, both programs predicted that the N-terminal region of AcrIIA5 would behave as a disordered region. The low complexity of the amino acid sequence and the presence of disorder-promoting motifs suggested that 20–30 residues at the N-terminus potentially remain disordered without well-defined secondary structures, albeit residues at the far end of the N-terminus exhibited less disorder probability than those near the inner core of the protein.

Secondary structure annotation and order parameters of AcrIIA5- Secondary structural information and predicted order parameters of AcrIIA5 were calculated using TALOS+ program based on the ^{1}H$_N$, ^{15}N, ^{13}Cα, ^{13}Cβ, and ^{13}C' chemical shifts (Figure 4A)[14]. The secondary structure prediction indicated that AcrIIA5 is comprised of two α-helices, seven β-strands, and a 3_{10} helix. The structure of AcrIIA5 determined by NMR spectroscopy was largely consistent with the

secondary structures predicted by the backbone torsion angles from the chemical shifts[20]. We note that the predicted order parameters from the random coil index suggest a significant flexibility at the N-terminal disordered region and the β3–β4 loop region (Figure 4B).

In summary, we report the optimal buffer condition and backbone chemical shift assignment of AcrIIA5. Both the amino acid sequence and NMR chemical shifts predict a long stretch of flexible disordered region at the N-terminus of AcrIIA5.

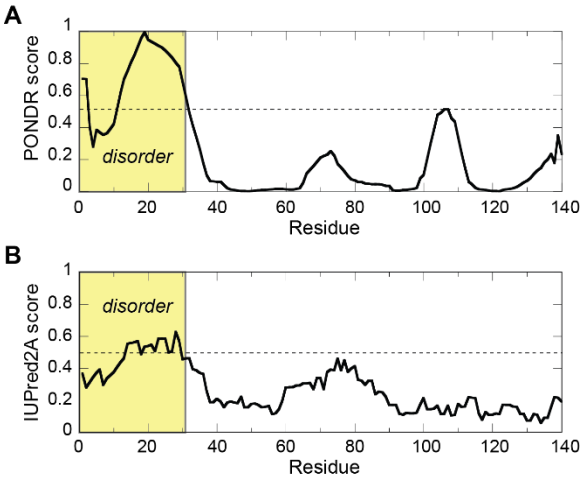

Figure 3. Disorder scores from the sequence-based prediction programs of (A) PONDR, and (B) IUPred2. The predicted disorder regions are highlighted in yellow shades and annotated.

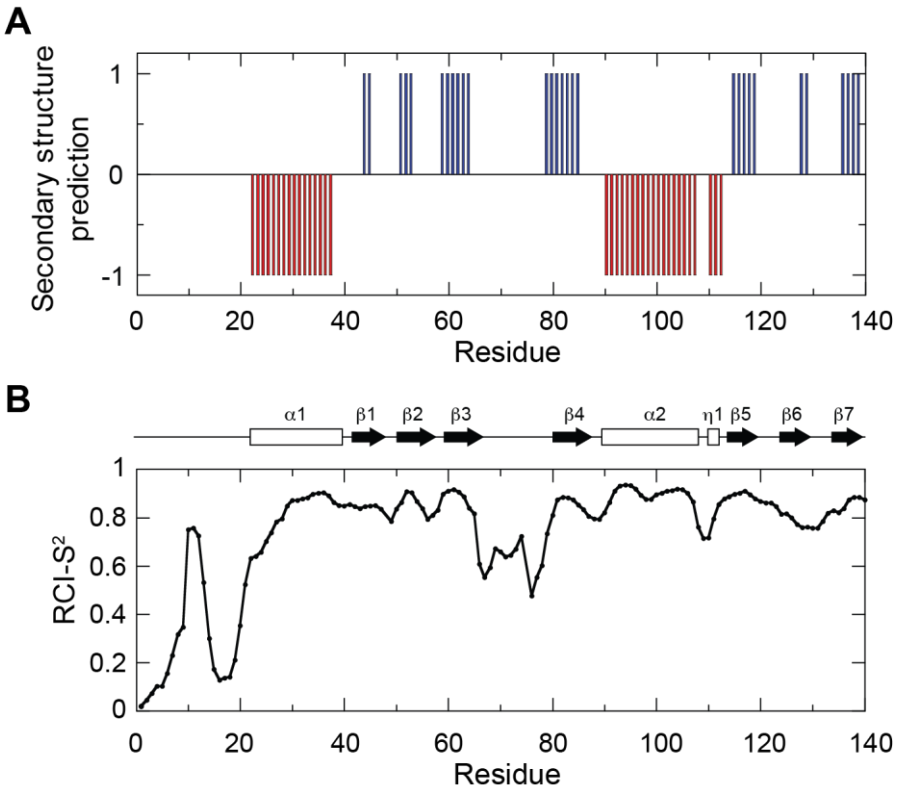

Figure 4. (A) Predicted secondary structures and (B) order parameters of AcrIIA5 based on backbone chemical shifts. Blue and red bars denote the predicted region of β-sheets and α-helices, respectively. The schematic representations of secondary structures are displayed at the top of (B). Order parameters were calculated via the random coil index using backbone chemical shifts.

Table 1. Backbone H_N, N, Cα, Cβ, and C' chemical shifts of AcrIIA5 (unit: ppm)

Residue	H_N	N	Cα	Cβ	C'	Residue	H_N	N	Cα	Cβ	C'
M1	8.438	122.56	55.70	32.94	175.45	K71	7.789	119.11	56.40	33.35	175.56
A2	8.350	125.73	52.37	19.42	177.14	Y72	7.910	119.42	58.17	38.30	175.44
Y3	8.156	119.58	58.05	38.85	176.45	H73	7.320	121.55	56.39		173.33
G4	8.336	110.45	45.47		174.15	D74					
K5	8.146	120.93	56.55	33.13	176.83	L75					
S6	8.330	116.45	58.79	63.94	174.61	E76					
R7	8.287	122.51	56.52	30.75	176.07	N77			53.92	38.29	175.66
Y8	8.113	120.14	58.02	38.76	175.62	G78	8.454	105.45	45.57		173.60
N9	8.245	120.32	53.42	39.02	175.76	R79	7.866	120.75	54.92	31.93	174.70
S10						L80	8.423	126.46	55.53	42.30	173.91
Y11						I81			58.97	37.93	174.12
R12						V82	8.706	126.34	60.22	32.06	174.13
K13	8.314	120.05	56.73	32.75	177.67	N83	8.935	126.47	53.15	43.08	173.38
R14	8.299	122.06	56.52	30.94	176.33	I84	9.457	126.90	60.01	39.77	174.67
S15	8.227	116.67	58.40	63.99	174.21	K85	7.879	127.12	56.48	33.19	176.36
F16	8.244	122.17	57.98	39.78	175.34	A86	8.420	130.29	52.10	22.92	174.67
N17	8.381	120.46	53.42	39.22	175.25	S87	8.337	113.49	56.69	64.64	175.98
R18			56.61	30.76	176.46	K88	8.486	124.32	57.99	32.00	177.30
S19	8.374	116.48	58.77	64.06	174.55	L89	7.608	116.98	56.43	41.16	177.35
N20	8.485	120.98	54.00	38.95	175.67	N90	8.108	114.66	52.80	40.58	175.42
K21	8.267	121.11	57.65	32.89	178.12	F91	7.401	118.43	58.76	38.44	176.73
Q22						V92	8.409	117.14	67.64	31.01	176.77
R23			57.06	30.55	177.24	D93	8.065	119.01	57.65	42.33	
R24	8.382	122.26	57.56	30.67	177.14	I94	8.200	117.55	65.38	37.81	178.27
E25	8.511	121.08	57.72	29.95	177.27	I95	8.137	121.40	66.29	38.19	178.20
Y26	8.213	121.35	59.70	38.64	176.47	E96	8.664	115.79	59.69	30.69	178.70
A27	8.232	123.08	54.36	18.74	179.28	N97	8.288	111.41	54.86	42.22	176.44
Q28	8.170	118.18	57.78	29.00	177.82	K98	8.293	117.75	56.05	35.25	177.01
E29	8.340	121.19	58.46	29.42	178.65	L99	8.255	121.28	57.65	42.85	178.17
M30			56.91	32.44	177.65	D100	8.639	118.66	57.91	39.64	178.63
D31	8.212	121.62	56.51	41.37	177.77	K101	7.731	117.43	58.23	32.55	178.70
R32	8.065	119.40	59.16	30.36	178.85	I102	7.280	119.03	65.49	38.75	177.14
L33	8.066	122.75	58.26	42.45	178.19	I103			65.22	37.69	176.77
E34	8.373	118.34	60.32	29.78	179.93	E104	7.847	116.64	59.06	29.74	178.68
K35	8.199	118.91	58.91	32.13	179.36	K105	6.860	114.90	59.56	33.24	179.10
A36	8.176	122.34	54.94	18.62	181.09	I106	7.823	117.78	64.05	37.39	177.80

Table 1. Backbone H_N, N, Cα, Cβ, and C' chemical shifts of AcrIIA5 (*continued*)

Residue	H_N	N	Cα	Cβ	C'	Residue	H_N	N	Cα	Cβ	C'
F37	8.226	116.68	61.74	39.21	178.22	D107	8.466	118.08	56.31	40.16	177.80
E38	7.843	120.66	59.06	29.58	177.39	K108	7.054	116.39	56.43	33.14	177.43
N39	7.389	113.86	53.15	39.91	174.28	L109	7.607	119.51	54.65	43.51	177.02
L40	7.266	121.93	53.41	41.98	175.72	D110	8.561	119.96	52.78	39.10	176.34
D41	8.495	124.31	56.10	41.46	176.94	L111	7.883	122.52	58.25	41.56	178.33
G42	8.641	114.39	45.72		171.72	D112	8.101	115.91	56.31	41.20	177.00
W43	7.166	118.06	56.64	30.98	175.94	K113	7.652	114.64	57.45	32.96	178.07
Y44	8.949	120.32	56.79	41.32	174.49	Y114	7.483	116.72	58.05	40.71	173.57
L45	8.595	122.05	53.45	44.71	177.94	R115	9.034	114.28	54.70	31.47	174.95
S46	8.802	118.59	58.04	64.71	176.97	F116	7.403	120.62	58.56	41.93	172.52
S47						I117	7.939	129.27	60.39	40.94	171.69
M48						N118	9.348	124.03	51.11	42.15	
K49						A119	9.787	133.60	50.99	18.91	176.60
D50			53.16	41.20	175.57	T120	8.460	117.55	63.37	69.39	173.36
S51	7.999	113.01	57.52	66.26	171.53	N121	9.950	126.76	52.00	38.33	173.44
A52	8.655	123.53	50.50	24.17	176.25	L122	9.254	118.93	56.86	39.30	175.50
Y53	9.212	118.14	56.44	43.01	172.69	E123			57.49	28.23	174.18
K54	8.222	118.37	56.02	30.88	174.23	H124	8.016	121.25	55.58	30.43	174.28
D55	8.860	125.82	54.24	41.67	175.97	D125	9.200	127.04	55.12	38.71	175.67
F56	8.931	126.50	58.76	39.91	176.60	I126	8.630	122.94	63.69	38.39	175.67
G57	9.177	114.86	46.95		175.50	K127	8.015	125.63	56.25	34.51	174.71
K58	7.850	120.62	57.32	32.90	175.34	C128	8.766	122.32	56.37	27.92	174.00
Y59	6.900	110.78	54.82	39.82	173.39	Y129	9.001	122.41	59.17	38.41	177.01
E60	9.014	121.42	54.82	33.76	175.46	Y130	8.364	124.87	60.02	40.02	177.87
I61	8.862	125.22	60.68	38.42	174.51	K131	8.690	122.31	58.21	33.92	177.21
R62	9.159	126.33	54.44	33.98	174.45	G132	9.241	110.76	45.45		172.83
L63	9.403	125.16	53.65	43.21	176.51	F133	7.561	115.85	56.69	44.19	174.80
S64	8.574	113.85	58.17	65.71	174.51	K134					
N65	9.292	124.20	52.34	39.50	176.10	T135			61.06	70.65	174.67
H66						K136	7.159	123.99	57.76	34.12	176.52
S67	8.140	116.06	58.90	63.76		K137	9.168	126.73	54.70	35.59	174.03
A68	8.642	127.45	52.31	19.63	177.13	E138	8.657	119.91	54.57	33.00	174.34
D69	8.326	119.80	54.69	41.06	176.14	V139	8.600	124.93	61.68	32.89	175.88
N70	8.248	118.04	54.09	38.52	175.15	I140	8.710	128.98	61.78	40.63	180.43

Acknowledgments

This work was supported by the Cooperative Research Program for Agriculture Science & Technology Development, Rural Development Administration (PJ01495901), and the Creative-Pioneering Researchers Program through Seoul National University (500-20200255). We thank the high-field NMR facility at the Korea Basic Science Institute, and the National Center for Inter-University Research Facilities of Seoul National University.

References

1. D. Deveau, J. E. Garneau, and S. Moineau, *Annu. Rev. Microbiol.* **64**, 475 (2010)
2. S. J. Brouns, *et al.*, *Science* **321**, 960 (2008)
3. E. V. Koonin, K. S. Makarova, and F. Zhang, *Curr. Opin. Microbiol.* **37**, 67 (2017)
4. W. Jiang and L. A. Marraffini, *Annu. Rev. Microbiol.* **69**, 209 (2015)
5. S. H. Sternberg and J. A. Doudna, *Mol. Cell* **568**, 568 (2015)
6. A. V. Wright, J. K. Nunez, and J. A. Doudna, *Cell* **164**, 29 (2016)
7. J. E. Samson, A. H. Magadán, M. Sabri, and S. Moineau, *Nat. Rev. Microbiol.* **11**, 675 (2013)
8. A. P. Hynes, *et al.*, *Nat. Microbiol.* **10**, 1374 (2017)
9. B. Garcia, *et al.*, *Cell Rep.* **29**, 1739 (2019)
10. G. Song, *et al.*, *Cell Rep.* **29**, 2579 (2019)
11. F. Delaglio, *et al.*, *J. Biomol. NMR* **6**, 277 (1995)
12. D. S. Garrett, R. Powers, A. M. Gronenborn, and G. M. Clore, *J. Magn. Reson.* **95**, 214 (1991)
13. B. A. Johnson and R. A. Blevins, *J. Biomol. NMR* **4**, 603 (1994)
14. Y. Shen, F. Delagio, G. Cornilescu, and A. Bax, *J. Biomol. NMR* **44**, 213 (2009)
15. K. S. Jo, *et al.*, *J. Kor. Magn. Reson. Soc.* **22**, 64 (2018)
16. M. D. Seo, *J. Kor. Magn. Reson. Soc.* **24**, 38 (2020)
17. G. W. Vuister, S. J. Kim, C. Wu, and A. Bax, *J. Am. Chem. Soc.* **116**, 9206 (1994)
18. P. Romero, *et al.*, *Proteins* **42**, 38 (2001)
19. B. Meszaros, G. Erdos, and Z. Dosztanyi, *Nucleic Acids Res.* **46**, W329 (2018)
20. S. Y. An, *et al.*, *Nucleic Acids Res.* **48**, 7584 (2020)